Impact of Longwall Coal Mining on Subsurface Stress Conditions – Will the Presence of Historic Coal Mines Exacerbate Induced Seismicity During Hydraulic Fracturing of Underlying Formations?

Dr. James P. Verdon

School of Earth Sciences,

University of Bristol

Report Commissioned by the Oil and Gas Authority

July 2018

Summary

- In some areas of the U.K., prospective shale formations are overlain by coal measures that have experienced significant historic longwall mining activity. Concerns have been raised as to the impacts of this historic mining on the underlying shales.
- This study investigates the geomechanical effects of longwall coal mining on the stress state in underlying shale layers, with particular focus on the critical state of stress acting on faults. Our model is loosely based on coal mining activities conducted at the Thoresby Colliery, as this is an extensively studied site.
- We find that the mining activities have a significant effect on the state of stress, with deformation extending to the ground surface, and up to 1 km below the mined panels.
- We find horizontal compressive stresses increase in the layers above the mined panels. This would act to close any vertical fractures in these layers, reducing vertical permeability and ensuring hydraulic isolation between the mined layers and any near-surface aquifers (as per Younger, 2016).
- We find that minimum critical pore pressures (the pore pressure increase required to reactivate an optimally-oriented fault) are reduced up to 300 m below the mined panels. Beyond this distance, the minimum critical pore pressure is not affected by the mining excavations.
- As a "first look" study, we have used simple, representative 2D models in a homogenous subsurface. The anticipated impact of these simplifications will be to overestimate the modelled deformation. More realistic models will be developed in future studies. Future studies will also examine the impact of mining-induced seismicity on underlying shale layers, and the impact of stress changes induced by hydraulic fracturing on the overlying coal layers.

Introduction

Concerns have been raised regarding the use of hydraulic fracturing for shale gas in areas that have experienced historic coal mining (Styles, 2018). Longwall coal mining in the East Midlands has taken place at depths of up to 1000 m. The Bowland Shale, which is currently a prospective target for shale gas operators, underlies the coal measures. Williamson and Evans (2018) estimate a variable distance of separation between the coal measures and the prospective Bowland Shale Formation of 300 – 1,300 m.

The proximity between historic coal mines and proposed hydraulic fracturing sites raises several questions. In this report we address the concern that historic mining activities could have altered the stress state on faults within the underlying shale layers, thereby increasing the probability of induced seismic activity during hydraulic fracturing.

To do this we build finite element numerical geomechanical models that simulate the deformation generated by longwall coal mining in the surrounding rock formations. We base our models loosely on the Thoresby Colliery, Nottinghamshire (Figure 1). This site has been extensively studied in the academic literature, focussing on episodes of mining-induced seismicity that occurred between 1989 – 1991 (Bishop et al., 1993; Styles et al., 1997) and between 2013 – 2014 (Verdon et al., 2018). Longwall coal mines have extracted coal from several seams, including the Deep Soft at 740 m depth; the Parkgate at approximately 780 m; the Top Hard at 650 m; and the High Hazels at 500 m (note all depths are approximate).

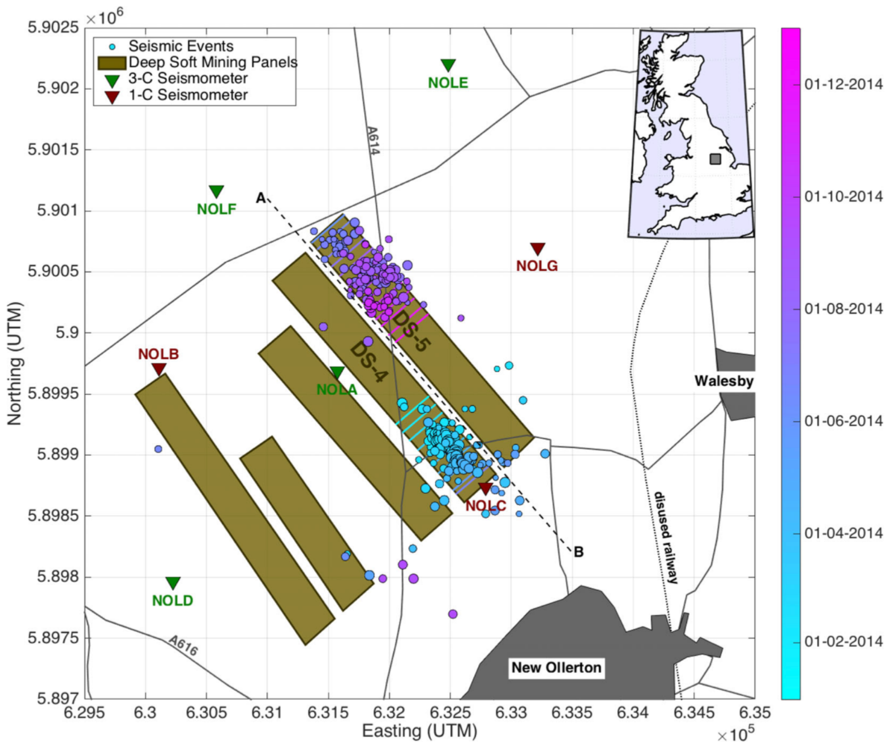

Figure 1: Seismicity induced by longwall mining at the Thoresby Colliery (from Verdon et al., 2018). Shaded dots show event locations, which track the positions of the mining front (shaded lines) within the longwall panels in the Deep Soft seam (brown rectangles). Inverted triangles show the positions of the surface seismometers used to detect and locate the events.

Method

We use the ADONIS finite element numerical modelling code (Mikola, 2017) to simulate the geomechanical deformation induced by longwall mining excavations. Figure 2 shows the model geometry we use. We simulate 3 parallel mining panels each in two separate seams, at depths of 500 m and 700 m. Both seams are simulated as 2 m thick. The mining panels are 300 m wide, with a spacing of 50 m between each panel. The models are 2-dimensional, so in effect represent longwall panels of infinite extent (and therefore would be expected to overestimate deformation).

A triangular mesh is used for the finite element modelling, with a maximum mesh size of 30 m, and local refinements of up to 0.4 m in proximity to the excavated panels. The model extends from the free surface to a depth of 3,000 m, extending laterally over 10,000 m (with the simulated panels in the centre of the model), sufficient to avoid any boundary effects. The model boundaries are simulated as "rollers" (i.e. the lateral edges can move in the *z* axis, but not laterally), while the model base can move in the *x* direction (i.e. laterally), but not in the *z* axis. The ground surface is modelled as a free surface that can move in any direction.

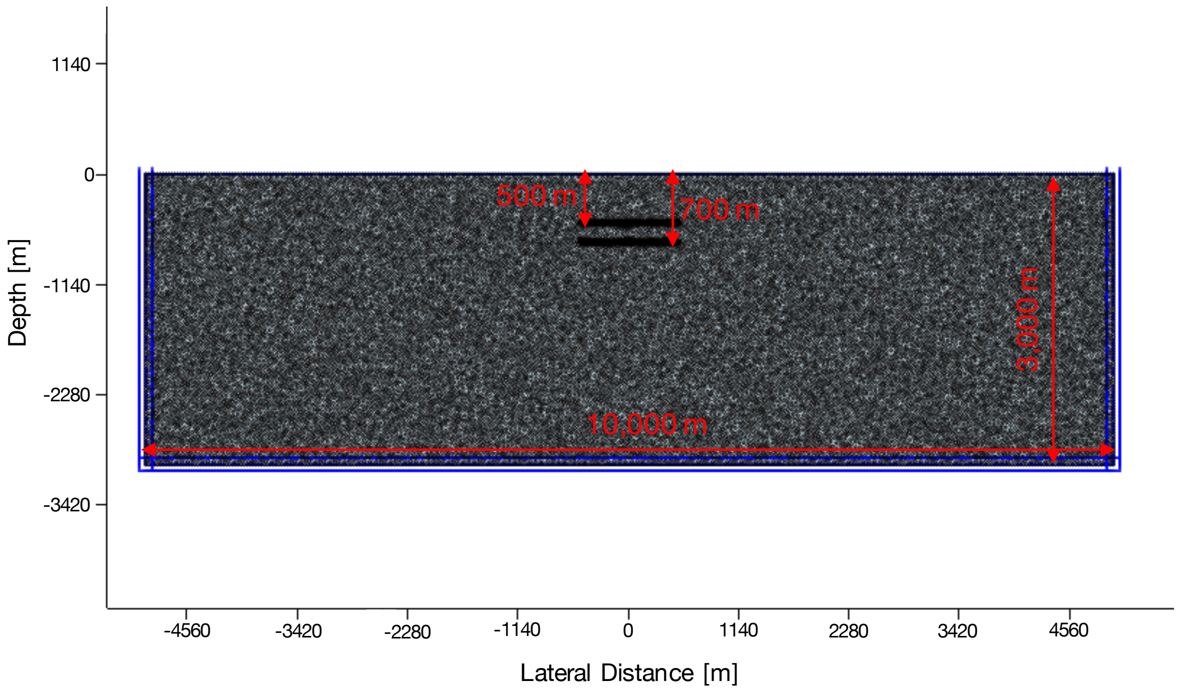

(a)

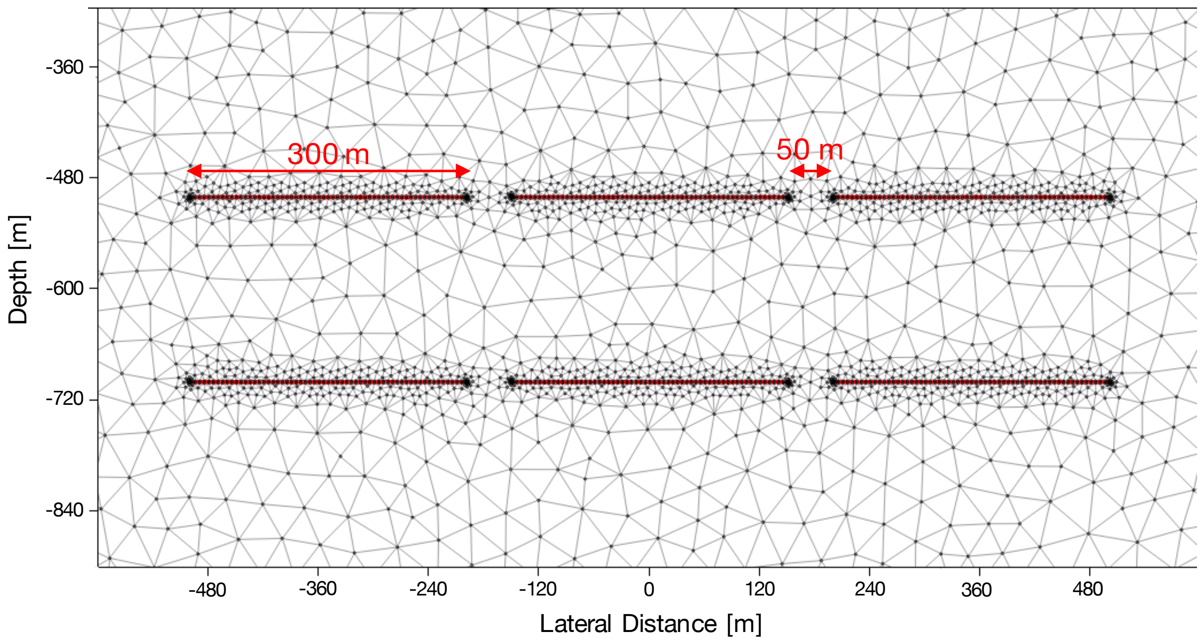

(b)

Figure 2: Modelling geometry: 3 longwall panels are simulated in each of two seams at depths of 500 and 700 m. (a) shows the full model, while (b) shows a zoomed-in area around the panels. The panels are 300 m wide, with an inter-panel spacing of 50 m. Both seams have a thickness of 2 m. A triangular mesh is used for the finite element model, with local grid refinements around the panels.

The rock mass is treated as a homogenous linear elastic material, with a bulk modulus of K = 3.3 GPa and shear modulus of μ = 2 GPa. In reality the rock mass in proximity of the mined panels would fail inelastically, forming a rubble zone or goaf, which would provide a degree of support the subsiding overburden. The neglect of this behaviour in our modelling produces a second mechanism by which the deformation might be overestimated here (e.g., Suchowerska Iwanec et al., 2016).

The initial *in situ* stress regime is treated as strike slip ($\sigma_{H_{max}} > \sigma_V > \sigma_{h_{min}}$), with stress gradients as a function of depth of $\sigma_{H_{max}}$ = 28.4 kPa/m, σ_V = 24.5 kPa/m, and $\sigma_{h_{min}}$ = 21.3 kPa/m. Following the inferences of Verdon et al. (2018), who used both World Stress Map data (Heidbach et al., 2016) and measurements of shear-wave splitting data made on earthquakes recorded at Thoresby, $\sigma_{H_{max}}$ is modelled as being parallel to the coal-mining direction (i.e. out of the plane of our 2D models), and $\sigma_{h_{min}}$ is perpendicular to the mining direction (i.e. in the *x* axis of our model).

These stress conditions are in agreement with the inferences made by Baptie (2009) using focal mechanisms of earthquakes from across the U.K.. We also note that earthquakes induced by hydraulic fracturing at Cuadrilla's Preese Hall well in 2011 (Clarke et al., 2014), and a natural event that occurred in proximity to Third Energy's Kirby Misperton site in September 2011 (Third Energy, 2017), all had strike-slip focal mechanisms.

Results

The simulated displacements and the changes in vertical and horizontal stresses are shown in Figures 3 – 5. As well as the 6 mining panel model described above, we also show the results for a single mining panel at 700 m depth. This allows us to examine the behaviour induced by a single panel, and to compare it to results from a multi-panel situation.

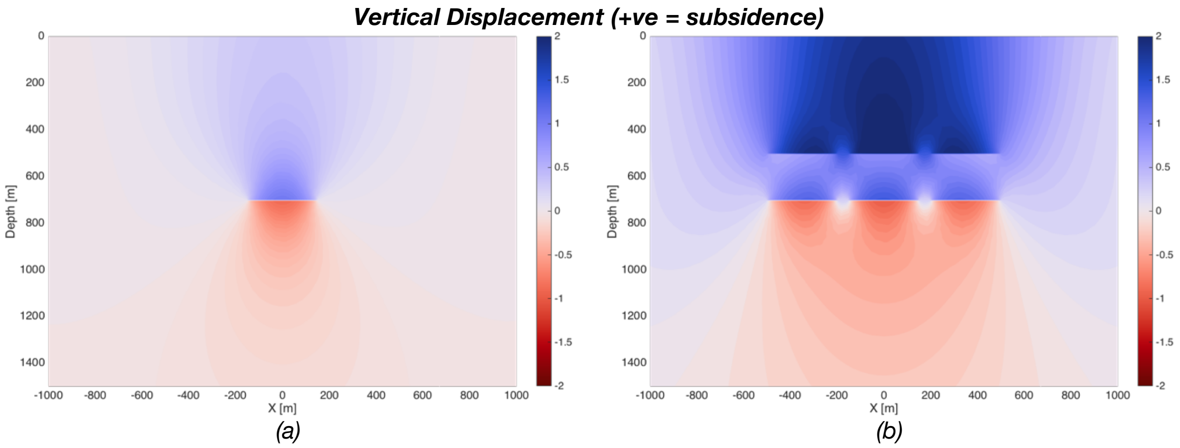

Figure 3: Modelled vertical displacement around (a) the one panel model, and (b) the multi-panel model. Positive values imply subsidence.

These results are in line with existing models of deformation around longwall coal mines (e.g., Kim et al., 1997; Larson and Whyatt, 2009; Rafiqul Islam et al., 2009; Suchowerska Iwanec et al., 2016). The overburden above the mine subsides, with a total of 0.35 m of surface subsidence above the single-panel model, which is 17% of the total coal thickness removed; and 2 m of subsidence above the multi-panel model, which is 50% of the total coal thickness removed (2 m in each modelled seam). The subsidence is largest directly above the seams and extends approximately 1 km laterally away from the seams. The rocks below the seams are displaced upwards (known as floor heave).

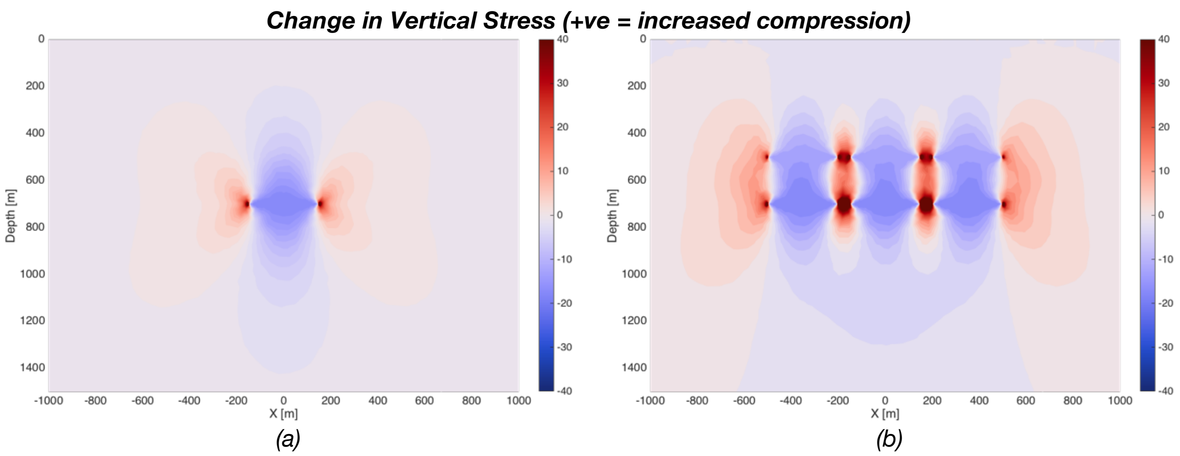

Figure 4: Modelled changes in vertical stress (in MPa) around (a) the one panel model, and (b) the multi-panel model. Positive values imply and increase in compressive stress.

The vertical stresses decrease (i.e. become less compressional) directly above and below the panels but increase at the sides of the panels as these areas support the overburden weight through stress arching (e.g., Segura et al., 2011). These stress changes extend to the surface, and approximately 1 km below the model.

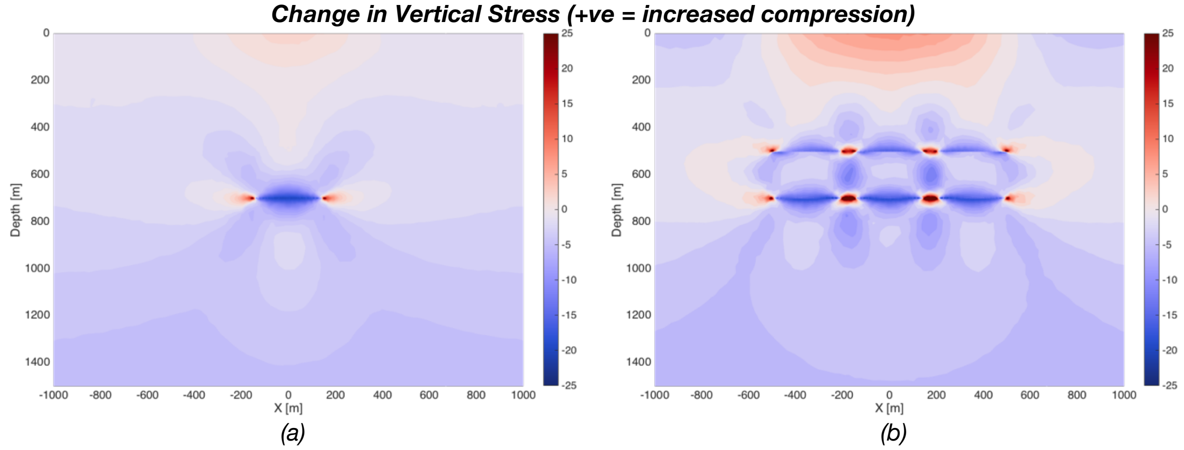

Figure 5: Modelled changes in horizontal stress (in MPa) around (a) the one panel model, and (b) the multi-panel model. Positive values imply and increase in compressive stress.

The horizontal stresses are also reduced immediately above the panels, but increase at shallower depths. Again, this matches with prior studies of mining-induced deformation, where increases in horizontal stresses at a given distance above the seam are noted: for example, Younger (2016) suggest a zone of horizontal compressive stress increase from a height of $W/3$ above the seam. Our models show horizontal stresses are increased from 575 m depth (125 m above the seam, or $W/2.4$) for the single panel model, and at 385 m depth (115 m above the shallower seam, or $W/2.6$) for the multi-panel model. At the sides of the panels the opposite effects are seen, with horizontal stresses increasing at the mined depths, but decreasing above and below the mine.

The impact of these horizontal stress increases above the mining panels would be to compress and close any vertical fractures. This would reduce the vertical permeability and thereby the ability of fluids to flow through these layers. Such mechanisms account for the ability of these mines to maintain hydraulic isolation from near-surface aquifers (e.g. Younger, 2016).

Implications for Fault Reactivation

We use Mohr-Coulomb (M-C) theory to assess the impacts of these stress changes on fault reactivation in underlying shale layers. Slip will occur on a fault if the shear stress τ resolved onto the fault plane exceeds the M-C threshold:

$$\tau > \phi \sigma_n + \chi,$$

where σ_n is the normal stress resolved onto the fault plane, ϕ is the coefficient of friction (assumed to be 0.6 throughout this study) and χ is the cohesion (assumed to be 0 throughout this study).

During hydraulic fracturing, the primary mechanism for fault reactivation is an increase in pore pressure which reduces the normal stress, thereby reducing the M-C threshold and allowing fault slip (i.e. a seismic event) to occur. As such, the stresses acting on a fault can be expressed in terms of the critical pore pressure P_C required to exceed the M-C threshold:

$$P_C = \sigma_n - \left(\frac{|\tau|}{\phi}\right).$$

A fault that is close to failure conditions will have a low P_C, implying that it could be reactivated easily with only a small increase in pore pressure.

For a given *in situ* stress tensor, P_C will be a function of the fault orientation, with faults that are oriented such that σ_n resolved onto the fault plane is minimised, while τ is maximised, being the closest to failure. We focus on this minimum value of P_C, because this represents the smallest pore pressure change that could induce seismic activity during hydraulic fracturing activities.

Figure 6 shows our modelled principal stresses directly below the mining panels (i.e. at x = 0). Because our models are 2D, the maximum horizontal stress, which acts into the plane of our model, is unchanged. Both the minimum horizontal stress and the vertical stress decrease below the panels, but the vertical stress is decreased by a greater amount, with the disturbance extending far deeper than the horizontal stress disturbance. Indeed, the decrease in vertical stress is such that in proximity to the mining panel the vertical stress becomes the minimum stress, and the stress regime switches from strike slip ($\sigma_{H_{max}} > \sigma_V > \sigma_{h_{min}}$) to reverse ($\sigma_{H_{max}} > \sigma_{h_{min}} > \sigma_V$). In reality, these stress changes account for the presence of dip-slip fault mechanisms associated with mining at Thoresby (Verdon et al., 2018), whereas the regional stress regime is strike-slip (e.g., Baptie, 2009; Heidbach, 2016).

The impact of these stress changes on the minimum fault criticality P_C is shown in Figure 7. P_C decreases in close proximity to the mining depths, implying that faults would be reactivated more easily. However, P_C returns to the initial conditions approximately 300 m below the seam. Below this depth, the simulated mining would not have increased the likelihood of fault reactivation.

Note that this separation distance is smaller than the overall extent of vertical stress reduction (Figure 6), which extends approximately 1 km below the mining panels. However, in a strike-slip regime the vertical stress is the intermediate stress, and therefore has no bearing on the maximum shear stresses experienced, which is determined by the relative magnitudes of the maximum and minimum horizontal stresses. As such, the reductions in vertical stress only begin to have an impact on the minimum P_C once it becomes less than the minimum horizontal stress, which in this study occurs at approximately 1000 m depth, or 300 m below the deepest mining panels.

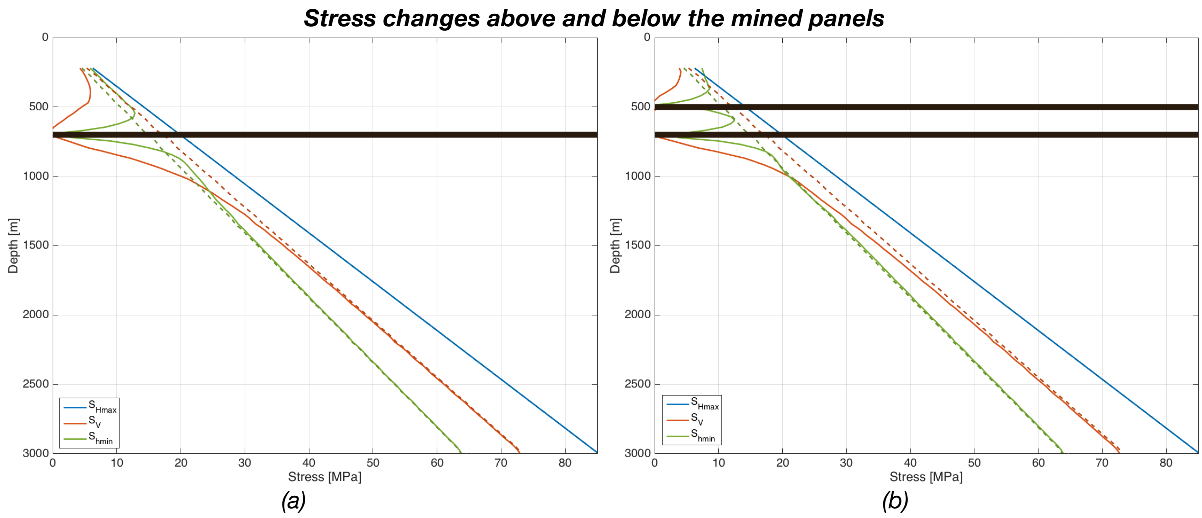

Figure 6: Modelled changes in principal stresses above and below the mined panels for (a) the one panel model, and (b) the multi-panel model. Dashed lines show the original stress gradients, while solid lines show the stresses after excavation.

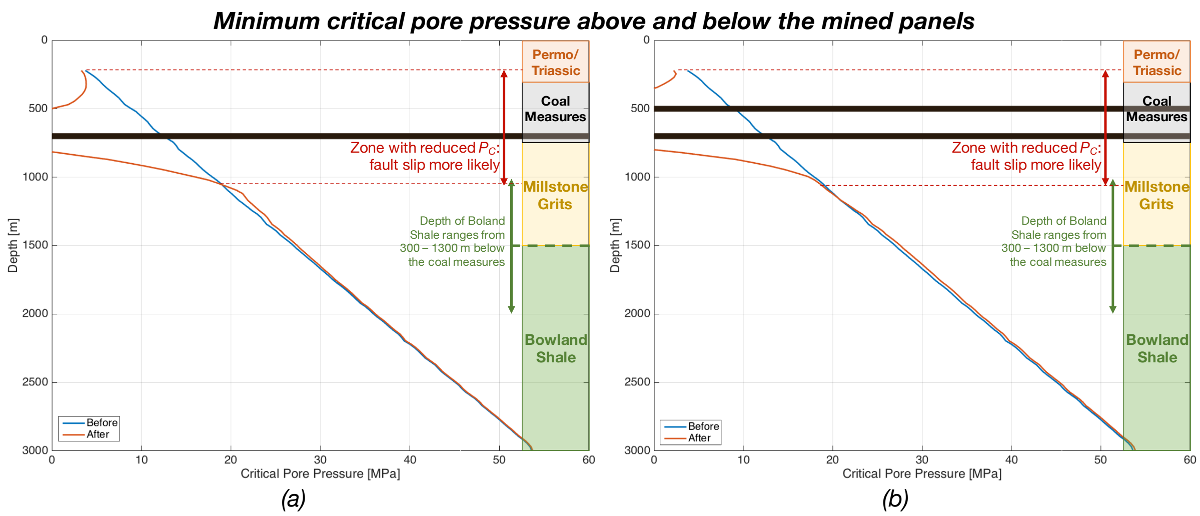

Figure 7: Modelled changes in minimum critical pore pressure P_C (in MPa) above and below the mined panels for (a) the one panel model, and (b) the multi-panel model. Lower P_C values imply a fault will slip more readily. A representative stratigraphic section is plotted to the right: the Bowland Shale Formation is between 300 – 1,300 m below the coal measures (Williamson and Evans, 2018). Note that this stratigraphy is shown for reference only, no mechanical stratigraphy was included in our model.

Further Work

This model represents a very simple "first look" into the impact of historic coal mining on hydraulic fracturing in underlying coal layers. As such, the models are extremely simple. Further work will be conducted along the following lines:

- The use of 3-dimensional models.

- The inclusion of realistic material properties that better simulate the inelastic behaviours that occur in proximity to the mined zones.
- The use of models that better represent the true mechanical stratigraphy of the different rock formations above and below the coal seams.
- Exploration of the parameter space to investigate how modelling parameters (geometries, material properties, *in situ* stress conditions, *et cetera*) affect the results.

Further work will also investigate the impact of mining-induced seismic events, such as those observed at Thoresby, on stresses in the underlying shale layers. We will also simulate impact of shale gas extraction on stresses in the coal strata, to investigate whether the stress changes induced by hydraulic fracturing have any impact of faults and fractures in the coal layers.

Conflicts of Interest

Given the potential significance of these issues with respect to the regulation of hydraulic fracturing, we note that J.P. Verdon has and continues to provide consulting services and advice regarding induced seismicity to shale gas operating companies in North America, the UK, and around the world. The views presented in this article are solely those of the author, who has received no input or contribution from shale gas operating companies in the writing of this report.

References

Baptie B., 2009. Seismogenesis and state of stress in the UK: *Tectonophysics* 482, 150-159.

Bishop I., P. Styles, M. Allen, 1993. Mining-induced seismicity in the Nottinghamshire coalfield: *Quart. J. Eng. Geol. Hydrogeol.* 26, 253–279.

Clarke H., L. Eisner, P. Styles, P. Turner, 2014. Felt seismicity associated with shale gas hydraulic fracturing: The first documented example in Europe: *Geophys. Res. Lett*. 41, 8308-8314.

Heidbach O., M. Rajabi, K. Reiter, M. Ziegler, WSM Team, 2016. World Stress Map Database Release 2016. *GFZ Data Services*.

Kim J-M., R.R. Parizek, D. Elsworth, 1997. Evaluation of fully-coupled strata deformation and groundwater flow in response to longwall mining: *Int. J. Rock Mech. Min. Sci.* 34, 1186-1199.

Larson M.K., and J.K. Whyatt, 2009. Critical review of numerical stress analysis tools for deep coal longwall panels under strong strata: *SME Annual Meeting, Denver Colorado*.

Mikola R.G., 2017. ADONIS: A Free Finite Element Analysis Software with an Interactive Graphical User Interface for Geoengineers: *GeoOttawa2017 Conference*.

Rafiqul Islam M., D. Hayashi, A.B.M. Kamruzzaman, 2009. Finite element modelling of stress distributions and problems for multi-slice longwall mining in Bangladesh, with special reference to the Barapukuria coal mine: *Int. J. Coal Geol.* 78, 91-109.

Segura J.M., Q.J. Fisher, A.J.L. Crook, M. Dutko, J.G. Yu, S. Skachkov, D.A. Angus, J.P. Verdon, J-M. Kendall, 2011. Reservoir stress path characterization and its implications for fluid-flow production simulations: *Pet. Geosci.* 17, 335-344.

Styles P., 2018a. Fracking and historic coal mining: their relationship and should they coincide? Accessed at https://www.keele.ac.uk/media/keeleuniversity/facnatsci/schgge/news/2018/Fracking%20and%20Mining-%20Styles%202018.pdf

Styles P., Bishop I., Toon S., 1997. Surface and borehole microseismic monitoring of mining-induced seismicity: In McCann D.M., M. Eddleston, P.J. Fenning, G.M. Reeves (eds), Modern Geophysics in Engineering Geology: *Geol. Soc. Eng. Geo. Spec. Pub.* 12, 315-326.

Suchowerska Iwanec A.M., J.P. Carter, J.P. Hambleton, 2016. Geomechanics of subsidence above single and multi-seam coal mining: *J. of Rock Mech. and Geotech. Eng.* 8, 304-313.

Third Energy, 2017. Hydraulic fracture plan for Well KM-8, Kirby Misperton Alpha wellsite: accessed at https://consult.environment-agency.gov.uk/onshore-oil-and-gas/third-energy-kirby-misperton-information-page/user_uploads/pre-op-2-hydraulic-fracture-plan-sept-17.pdf.

Verdon J.P., J-M. Kendall, A. Butcher, R. Luckett, B.J. Baptie, 2018. Seismicity induced by longwall coal mining at the Thorseby Colliery, Nottinghamshire, U.K.: *Geophys. J. Int.* 212, 942-954.

Williamson J.P. and D.J. Evans, 2018. First results of studies on the separation of the Bowland-Hodder shale unit from coal mining activity in the East Midlands: *Commissioned Report CR/17/078, British Geological Survey*.

Younger P.L., 2016. How can we be sure fracking will not pollute aquifers? Lessons from a major longwall coal mining analogue (Selby, Yorkshire, UK): *Earth and Env. Sci. Trans. Royal Soc. of Edin.* 106, 89-113.